Phase separation in coupled chaotic maps on fractal networks

K. Tucci,[1] M. G. Cosenza,[2] and O. Alvarez-Llamoza[3]
[1]*SUMA-CESIMO, Universidad de Los Andes, Mérida, Venezuela*
[2]*Centro de Astrofísica Teórica, Facultad de Ciencias, Universidad de Los Andes, Apartado Postal 26 La Hechicera, Mérida 5251, Venezuela*
[3]*Departamento de Física, FACYT, Universidad de Carabobo, Valencia, Venezuela*
(Received 1 May 2003; published 21 August 2003)

The phase ordering dynamics of coupled chaotic maps on fractal networks is investigated. The statistical properties of the systems are characterized by means of the persistence probability of equivalent spin variables that define the phases. The persistence saturates and phase domains freeze for all values of the coupling parameter as a consequence of the fractal structure of the networks, in contrast to the phase transition behavior previously observed in regular Euclidean lattices. Several discontinuities and other features found in the saturation persistence curve as a function of the coupling are explained in terms of changes of stability of local phase configurations on the fractals.

DOI: 10.1103/PhysRevE.68.027202 PACS number(s): 05.45.−a, 89.75.Kd

Coupled map lattices have provided fruitful and computationally efficient models for the study of a variety of dynamical processes in spatially distributed systems [1]. The discrete-space character of coupled map systems makes them specially appropriate for the investigation of spatiotemporal dynamics on nonuniform or complex networks. Phenomena, such as pattern formation, spatiotemporal intermittency, nontrivial collective behavior, synchronization, etc., have been extensively studied in coupled map systems defined on fractal lattices [2], hierarchical structures [3], trees [4], random graphs [5], small-world networks [6], and scale-free networks [7].

Recently, there has been much interest in the study of the phase-ordering properties of systems of coupled chaotic maps and their relationship with the Ising models in statistical physics [8–14]. These works have invariably assumed the phase competition dynamics taking place on a uniform Euclidean space; however, in many physical situations the medium that supports the dynamics can be nonuniform on some length scales. The nonuniformity may be due to the intrinsic heterogeneous nature of the substratum, such as porous or fractured media, or it may arise from random fluctuations in the medium. This paper investigates the phenomenon of phase ordering in coupled chaotic maps on fractal networks as a model for studying this phenomenon on nonuniform media. The class of fractal networks being considered corresponds to generalized Sierpinski gaskets (GSG) embedded in Euclidean spaces of arbitrary dimension d [2]. In particular, this model of coupled maps on fractal networks yields a situation to explore the role that the connectivity of the underlying lattice plays on the statistical properties of phase ordering processes in nonlinear coupled systems.

Deterministic fractal networks, such as GSG, can be generated in any d-dimensional Euclidean space as follows [2]. At the nth level of construction, the fractal consists of $N=(d+1)^n$ d-dimensional hypertetrahedral cells whose coordinates can be specified by a sequence $(\alpha_1\alpha_2\ldots\alpha_n)$, where α_m can take any value in a set of $d+1$ different symbols which can be chosen to be $\{0,1,\ldots,d\}$. At level $n+1$, each cell $(\alpha_1\alpha_2\ldots\alpha_n)$ splits into $d+1$ cells scaled down by a longitudinal factor of 2, and which are now labeled by $(\alpha_1\alpha_2\ldots\alpha_n\alpha_{n+1})$, where the first n symbols of the sequence are the same as the parent cell. Given this construction rule, the fractal dimension of the GSG is $d_f=\log(d+1)/\log 2$. A label $(\alpha_1\alpha_2\ldots\alpha_n)$ can be written as $(\alpha_1\alpha_2\ldots\alpha_{n-s}\alpha_{n-s+1}^s)$ for some $s\in\{1,2,\ldots,n\}$, where α_i^s means the sequence of s identical symbols α_i. The cell with this label has a neighborhood $\mathcal{N}_{(\alpha_1\alpha_2\ldots\alpha_n)}$ with $d+1$ elements labeled by $[\alpha_1\ldots\alpha_{n-1}(\alpha_n+j)]$ $(j=1,2,\ldots,d)$ and $(\alpha_1\ldots\alpha_{n-s+1}\alpha_{n-s}^s)$, where the addition α_i+j is defined as modulo $(d+1)$. If $s=n$, then the cell is one of the $d+1$ vertices of the gasket, labeled by (α_1^n), and it has only d neighbors belonging to the same parent cell. An integer index, $i=0,1,\ldots,(d+1)^n-1$, can be assigned to each cell of the lattice at the level of construction n by the rule $i=\sum_{m=1}^{n}\alpha_m(d+1)^{n-m}$.

The equations describing the dynamics of the diffusively coupled map system defined on these fractal networks at level of construction n, embedded in a d-dimensional Euclidean space, are

$$x_{t+1}(\alpha_1\ldots\alpha_n)=(1-\epsilon)f(x_t(\alpha_1\ldots\alpha_n))+\frac{\epsilon}{d+1}\times\sum_{(\beta_1\ldots\beta_n)\in\mathcal{N}_{(\alpha_1\ldots\alpha_n)}}f(x_t(\beta_1\ldots\beta_n)),\quad(1)$$

where $x_t(\alpha_1\ldots\alpha_n)$ gives the state of the cell $(\alpha_1\ldots\alpha_n)$ at discrete time t; $(\alpha_1\ldots\alpha_n)$ and $(\beta_1\ldots\beta_n)$ label the $(d+1)^n$ cells on the gasket; ϵ is a parameter measuring the coupling strength between neighboring sites, and $f(x)$ is a nonlinear function that expresses the local dynamics. Equation (1) also applies to the $(d+1)$ vertex cells of the fractal network, except that the coefficient of the sum is ϵ/d, since each of these cells have d neighbors.

As local dynamics, we assume a piecewise linear, odd map [10]

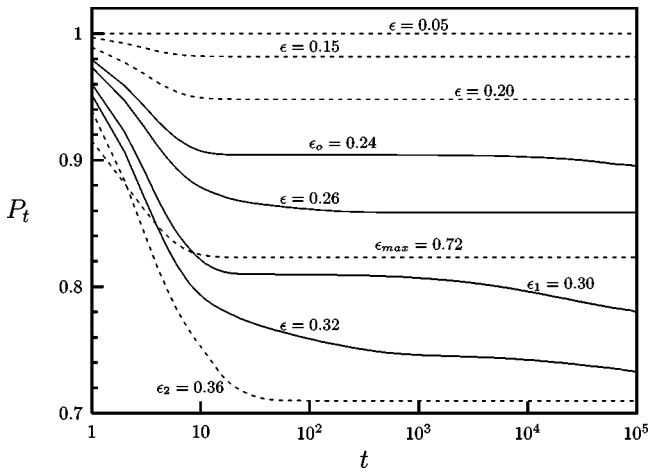

FIG. 1. Persistence probability as a function of time for the Sierpínski gasket embedded in Euclidean dimension $d=3$ for different values of the coupling ϵ. The lattice size is $N=4^9$. Dotted curves correspond to values of ϵ for which P_t reaches its saturation value quickly.

$$f(x)=\begin{cases} -2\mu/3-\mu x & \text{if } x\in[-1,-1/3], \\ \mu x & \text{if } x\in[-1/3,1/3], \\ 2\mu/3-\mu x & \text{if } x\in[1/3,1], \end{cases} \tag{2}$$

which for $\mu=3$ becomes the chaotic map introduced by Miller and Huse [8]. When the parameter $\mu\in[1,2]$, the map possesses two symmetric chaotic attractors contained in the intervals $I^{\pm}=[\pm\mu(2-\mu)/3,\pm\mu/3]$, and separated by a gap $I^{o}=[-\mu(2-\mu)/3,\mu(2-\mu)/3]$. For values of μ close to 2, the size of the chaotic intervals is larger than the gap. Then the local states have two well-defined symmetric phases that can be characterized by spin variables defined as the sign of the state at time t, $\sigma_t(\alpha_1 \ldots \alpha_n)=\mathrm{sign}[x_t(\alpha_1 \ldots \alpha_n)]$.

To study the phase-ordering phenomenon of the coupled maps on fractal networks, we fix the local map parameter at the value $\mu=1.9$ and set the initial condition as follows: if the number of cells $(d+1)^n$ in a lattice is even (d odd), exactly one half of the sites are randomly chosen and are assigned random values uniformly distributed on the interval I^+, while the other half are similarly assigned values on I^-. If the number of cells in a lattice is odd (d even), then the state of the remaining cell is assigned at random on either interval I^+ or I^-.

The statistical properties of the phase-ordering process on the fractal networks can be characterized by using the persistence probability P_t, defined as the fraction of cells that have not changed sign up to time t [15]. Figure 1 shows P_t as a function of time for the GSG embedded in $d=3$, for several values of the coupling parameter. For some ranges of the coupling, the persistence saturates in a few iterations, while for some other ranges of ϵ, P_t reaches its saturation value more slowly. In contrast, in regular Euclidean lattices the persistence saturates for small couplings, while it decays algebraically in time for coupling strengths greater than some critical value [10].

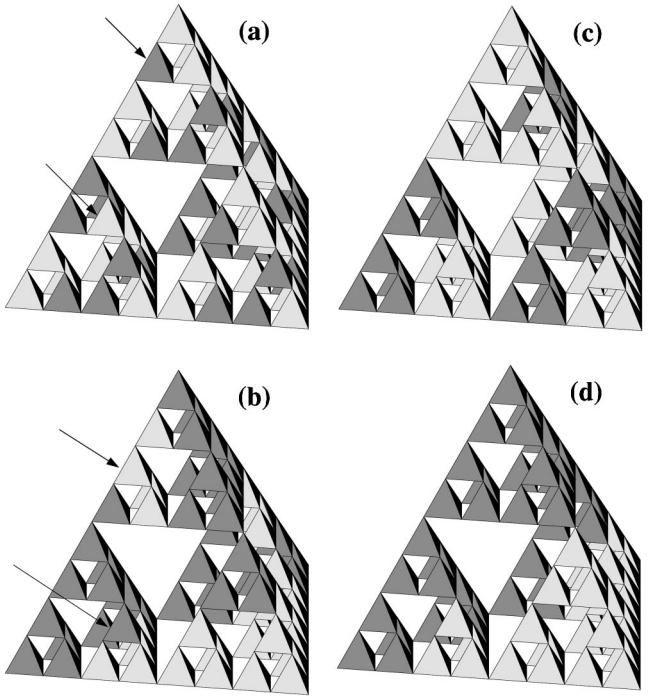

FIG. 2. Phase separation on the GSG embedded in Euclidean dimension $d=3$ at a level of construction $n=3$, for several values of the coupling. The dark (light) color corresponds to the positive (negative) phase. Arrows signal local configurations described in the text. (a) $\epsilon=0.20$, (b) $\epsilon=0.26$, (c) $\epsilon=0.36$, (d) $\epsilon=0.72$.

The domains formed by the two phases on fractal lattices reach a frozen configuration for all values of the coupling $\epsilon\in[0,1]$. Figure 2 shows the asymptotic patterns of the phase separation process on a GSG embedded in $d=3$ at level of construction $n=3$, for several values of the coupling. Note that the configuration of the blocked phase domains changes as the coupling is varied. The domain configurations can be characterized by the fraction of sites in a given phase that have k neighbors in that same phase at time t, denoted by $F_t(k)$, with $k=0,1,\ldots,d+1$. For example, consider the pattern displayed in Fig. 2(a) where there are several sites in one phase, as those indicated by arrows, having all of their four neighbors in the opposite phase. Thus, the asymptotic fraction $F_\infty(0)$ is greater than 0 in this case. In Fig. 2(b), as ϵ increases, $F_\infty(0)$ becomes 0, but $F_\infty(1)$ is finite, since there are sites in one phase, as those signaled by arrows, having just one neighbor in that same phase.

The relationship between the asymptotic behavior of the persistence and the frozen domain configurations on fractals becomes manifest in Fig. 3(a), which shows the saturation value of the persistence, P_∞, as well as the fractions $F_\infty(0)$, $F_\infty(1)$, and $F_\infty(2)$ as functions of the coupling parameter for the GSG embedded in Euclidean dimension $d=3$. Several discontinuities are observed in the curve of P_∞ in Fig. 3(a). The first discontinuity of P_∞ occurs at the value of the coupling $\epsilon_o=0.24$ where the fraction $F_\infty(0)$ vanishes. This implies that local blocked configurations where a site has no neighbors in its same phase, as those indicated in Fig. 2(a), become unstable at the value of coupling ϵ_o. The second discontinuity of P_∞ takes place at the value of coupling

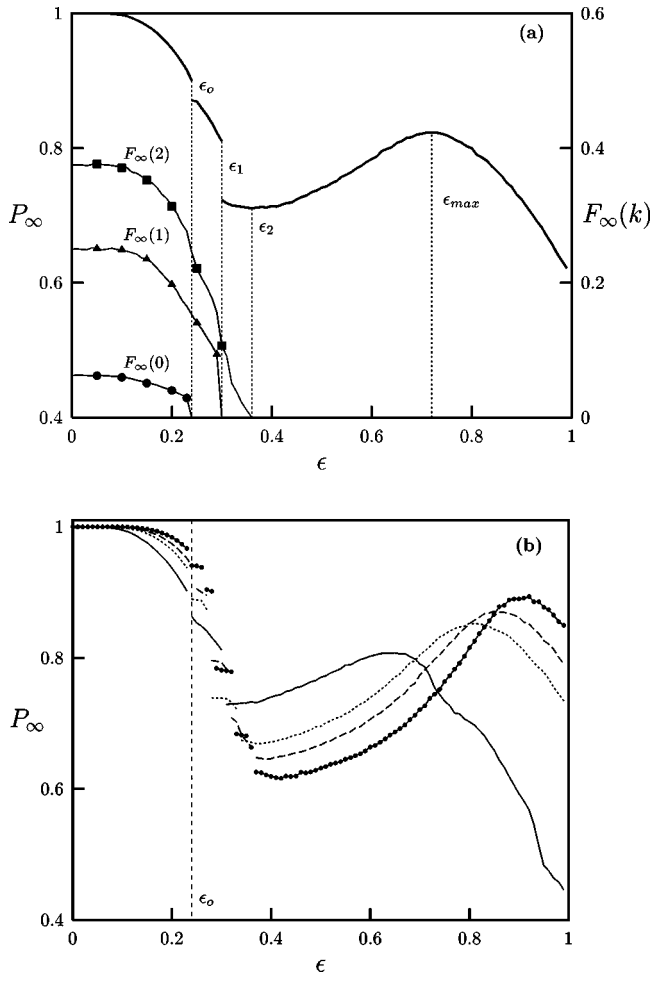

FIG. 3. (a) Left scale: saturation persistence P_∞ as a function of ϵ for the GSG embedded in Euclidean dimension $d=3$, represented by the thick dark line. The values $\epsilon_o, \epsilon_1, \epsilon_2$, and ϵ_{max} are indicated by dotted vertical lines. Right scale: fraction $F_t(k)$ vs ϵ. Circles, $F_\infty(0)$; triangles, $F_\infty(1)$; squares, $F_\infty(2)$. The lattice size is $N=4^9$. (b) P_∞ as a function of ϵ for GSG embedded in different Euclidean dimensions d. Continuous line: $d=2$, $N=3^{11}$; dotted line line: $d=5$, $N=6^7$; dashed line: $d=7$, $N=8^6$; circle line: $d=11$, $N=12^5$. The first discontinuity at $\epsilon_o=0.24$, common to all lattices, is indicated.

$\epsilon_1=0.30$ where $F_\infty(1)$ becomes 0, and it is related to the loss of stability of local frozen domain configurations as those signaled in Fig. 2(b). In addition, P_∞ reaches a minimum at the value of coupling $\epsilon_2=0.36$, where the fraction $F_\infty(2)$ decays to 0. For $\epsilon>\epsilon_2$, the domains of the two phases grow in size, as seen in Figs. 2(c) and 2(d). The phase domains also form faster, reducing the number of phase switching of the elements and, therefore, producing an increment in the saturation values P_∞ up to a maximum occurring at $\epsilon_{max}=0.72$.

A similar behavior is observed for all the fractal networks embedded in different Euclidean dimensions d. Figure 3(b) shows the saturation persistence P_∞ as a function of ϵ for GSG associated to different d. The discontinuities on each curve are related to the loss of stability of the configurations where one local element has a majority of its neighbors in the opposite phase. The number of those configurations is $J=\text{nint}[(d+1)/2]$, where nint(x) rounds x to its nearest integer. These J discontinuities take place at increasing values of the coupling ϵ_k for which the asymptotic fractions $F_\infty(k)$ vanish, with $k<J$. The first discontinuity is related to the vanishing of the fraction $F_\infty(0)$ at the value $\epsilon_o=0.24$, independent of the embedding dimension d. This independence is due to the presence of the normalization factor $(d+1)^{-1}$ in the coupling term in Eq. (1) for all the lattices. For embedding dimensions d odd, there occurs a minimum of P_∞ when the fraction $F_\infty(J)$ becomes 0. In those cases the local configurations losing stability are those consisting of a site with half of its neighbors in one phase and the other half in the opposite phase. These local configurations are symmetric, in the sense that a change of phase of that site does not alter the phase composition of its neighborhood. These symmetric configurations cannot happen in GSG associated to d even, and for those networks the minimum of P_∞ coincides with the last discontinuity that takes place when $F_\infty(J-1)$ vanishes.

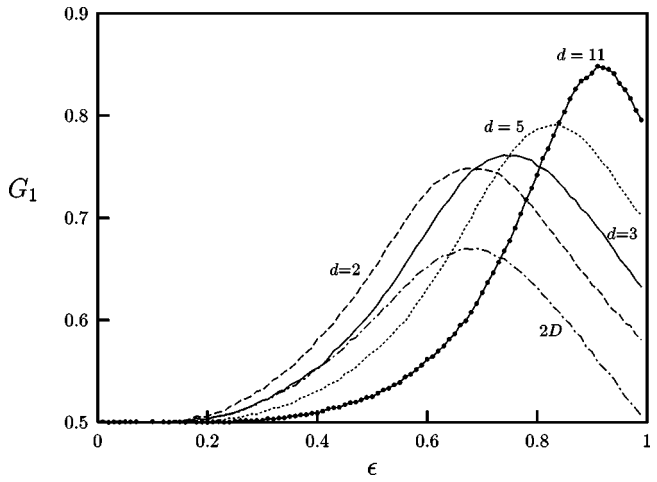

FIG. 4. G_1 as a function of ϵ for GSG embedded in different d. Dashed line: $d=2$; continuous line: $d=3$; dotted line: $d=5$; circle line: $d=11$. Sizes are the same as in Fig. 3. Dotted-dashed line represents G_1 for a two-dimensional regular lattice $(2D)$.

Note that for each fractal lattice there is a value of the coupling ϵ_{max} where a maximum of P_∞ is observed. The origin of such maximum can be analyzed through the average fraction of neighboring pairs that have opposite phases at time t, defined as

$$G_t=1-\frac{1}{N(d+1)}\sum_{i=1}^{N}\left(\sum_{j\in\mathcal{N}_i}\delta(\sigma_t(i),\sigma_t(j))\right), \qquad (3)$$

where $\delta(\sigma_t(i),\sigma_t(j))=1$ if $\sigma_t(i)=\sigma_t(j)$, and $\delta(\sigma_t(i),\sigma_t(j))=0$ otherwise. In Fig. 4 we show G_1 as a function of the parameter ϵ for different fractal lattices. The maximum of G_1 for each lattice takes place at the value ϵ_{max} at which the corresponding curve of P_∞ reaches a maximum. When G_1 is maximum the probability that there exist cells in one phase having all of their neighbors in the opposite phase at the first iteration is also maximum. Therefore, for the

value of coupling ϵ_{max}, there is a greater chance that at the next iteration such cells change phase instead of their neighbors, yielding more stable domains with fewer elements of the network having to switch their initial phase. Consequently, the persistence probability, which measures the number of elements that have not changed phases, is maximum at that time. Since the domains that are being formed are the most stable, in successive times the persistence will sustain a maximum value for the value of coupling ϵ_{max} corresponding to each lattice. For $\epsilon > \epsilon_{max}$ the coupling is strong enough to induce transient changes in the phase of elements having the majority of their neighbors in that same phase and, therefore, producing lower values of P_∞.

The local effect captured by the quantity G_1 in fractal lattices also appears in regular Euclidean lattices, although the asymptotic behavior of the persistence is different in those two network topologies. Figure 4 includes the calculation of G_1 as a function of ϵ for a two-dimensional regular lattice; the maximum of G_1 in this case occurs at $\epsilon_{max} = 0.67$. This is the critical value of the coupling parameter found in Ref. [10], after proper normalization, for the phase-ordering transition in the scaling behavior of the persistence in a two-dimensional Euclidean lattice. At $\epsilon = 0.67$ the blocked states in the two-dimensional regular lattice give place to growing domains of the two phases, separated by a continuous interface. The interface motion is driven by curvature effects that cause changes of phase in many elements of the system and, therefore, a temporal decay in the persistence probability [11]. In general, in regular Euclidean lattices the ratio between the length of the interface to the size of a domain decays as r^{-1}, where r is the average radius of the domain. On the other hand, in the fractal networks the interface consists of a few disconnected cells separating large domains, and no curvature can be defined. Because of the self-similarity of the structure the number of elements in a domain grows as $r^{d_f} = (d+1)^l$, where l is an integer, while the size of the interface is of the order of $(d+1)$, independent of the domain sizes. Thus, the ratio of the interface to domain size decreases as $r^{-d_f(l-1)/l}$ in the fractals. This decay is much faster than in regular Euclidean lattices and accelerates with increasing domain size, forming stable separated phase domains. As a consequence, domains always freeze on the fractal networks and the phase transition observed in the temporal behavior of the persistence in regular Euclidean lattices does not occur in fractals. Frozen domain configurations and absence of this phase transition may also be expected in similar models of coupled chaotic maps on other nonuniform lattices such as random graphs, small-world networks, and scale-free networks.

In summary, we have found that phase domains in chaotic maps coupled on fractal networks always reach a frozen configuration, causing the saturation of the persistence in time for all values of the coupling parameter, in contrast to the phase-transition behavior of the persistence observed in Euclidean regular lattices. The fractal nature of the spatial support is also reflected in the discontinuities observed in the P_∞ vs ϵ curves in Fig. 3. The phase configurations of the local neighborhoods have similar transient manifestations in fractal networks and in Euclidean regular lattices, as seen in the emergence of a maximum of G_1 at a value of coupling ϵ_{max}. However, the asymptotic and global properties of the phase ordering process on these two network topologies are quite different, even when the number of local connections in the neighborhood is the same, as it happens for the two-dimensional Euclidean lattice and the GSG embedded in $d = 3$. The necessary correlations between elements for building complex collective dynamics are more likely to occur in the denser Euclidean lattices. These results suggest that the topology of the network and not the number of local connections or the dimensionality of the space determine the asymptotic collective behaviors that may emerge on networks of coupled chaotic elements.

This work was supported by Consejo de Desarrollo Científico, Humanístico y Tecnológico, Universidad de Los Andes, Mérida, Venezuela.

[1] Chaos **2**, 279 (1992), focus issue on coupled map lattices, edited by K. Kaneko.
[2] M.G. Cosenza and R. Kapral, Chaos **4**, 99 (1994).
[3] P.M. Gade, H. A Cerdeira, and R. Ramaswamy, Phys. Rev. E **52**, 2478 (1995).
[4] M.G. Cosenza and K. Tucci, Phys. Rev. E **64**, 026208 (2001).
[5] D. Volchenkov, S. Sequeira, Ph. Blanchard, and M.G. Cosenza, Stoch. Dyn. **2**, 203 (2002).
[6] M.G. Cosenza and K. Tucci, Phys. Rev. E **65**, 036223 (2002).
[7] S. Jalan and R.E. Amritkar, Phys. Rev. Lett. **90**, 014101 (2003).
[8] J. Miller and D.A. Huse, Phys. Rev. E **48**, 2528 (1993).
[9] C. O'Hern, D. Egolf, and H.S. Greenside, Phys. Rev. E **53**, 3374 (1996).
[10] A. Lemaitre and H. Chaté, Phys. Rev. Lett. **82**, 1140 (1999).
[11] J. Kockelkoren, A. Lemaitre, and H. Chaté, Physica A **288**, 326 (2000).
[12] W. Wang, Z. Liu, and B. Hu, Phys. Rev. Lett. **84**, 2610 (2000).
[13] L. Angelini, M. Pellicoro, and S. Stramaglia, Phys. Lett. A **285**, 293 (2001).
[14] F. Schmüser, W. Just, and H. Kantz, Phys. Rev. E **61**, 3675 (2000).
[15] B. Derrida, A.J. Bray, and C. Godreche, J. Phys. A **27**, 357 (1994).